Science and Innovation of Advanced Materials

The Materials Research Society of Thailand

Research Article

Microstructural and Interfacial Designs of Dual-Phase Oxygen Permeable Membranes for Oxygen Separation Application

Aunsaya Eksatit[1,2], Kento Ishii[2], Masako Uematsu[1,2], Lihong Liu[2], Kiyoshi Kobayashi[2], Tohru S. Suzuki[2], Tetsuo Uchikoshi[1,2,*]

[1] Graduate School of Chemical Sciences and Engineering, Hokkaido University, Kita-ku, Sapporo, Hokkaido 060-0808, Japan
[2] Research Center for Functional Materials, National Institute for Materials Science (NIMS), Tsukuba, Ibaraki 305-0047, Japan

* Corresponding author e-mail: uchikoshi.tetsuo@nims.go.jp

Received: *August 20th, 2021* | ***Revised:*** *October 29th, 2021* | ***Accepted:*** *October 30th, 2021*

Abstract: A new and simple fabrication method by using a vacuum infiltration and spark plasma sintering (SPS) process for a dual-phase oxygen separation membrane consisting of electronic and ion-conducting phases has been presented. This method is able to form a co-continuous microstructure of the dual-phase and can realize the theoretical structure of a dual-phase membrane that has high efficient conducting paths of both carriers. The slurry of oxide ion-conducting materials (8 mol% yttria-stabilized zirconia (8YSZ)) was filled in a porous body of electron-conducting materials (carbon felt and nickel foam) by a vacuum infiltration process, then sintered by SPS process under the applied pressure of 80 MPa. The YSZ-based dual-phase membrane with a gas-tight and co-continuous structure, high chemical compatibility, and good phase stability was successfully fabricated. Finally, the ability to separate oxygen gas from air of a selected sample, the YSZ-nickel foam dual-phase membrane sintered at 1200 °C was investigated. The highest oxygen permeation flux of 0.21 ml/min·cm² was achieved at 800 °C, suggesting that this new processing route could be used for fabricating the oxygen separation membrane.

Keywords: Dual-phase membrane, Composite materials, Spark plasma sintering, Yttria-stabilized zirconia

1. Introduction

Oxygen is one of the most important industrial gases widely used in various fields. Generally, oxygen is produced by separation from air. The methods to separate oxygen from air can be classified into three types which are cryogenic separation, adsorption separation and membrane separation. First, the cryogenic separation method, which is a method using the difference in the boiling points of the air components, is a commercialized technology for the large-scale production of pure oxygen. An adsorption separation is the method in which the adsorbent was used to separate an oxygen gas by adsorption and desorption cycle. The oxygen separation membrane is a method in which sieving a specific gas by the differences in micropore size of material with gas molecular size [1]. In the present, a household

oxygen supplier which is a small to medium scale oxygen separation production has been attention [2]. Among these three methods, an oxygen separation membrane is suitable for the small-scale production. Among a various types of separation membrane, the separation membrane using a mixed oxide ion-electron conductor (MIECs)-based membrane is a promising oxygen separation membrane that electrochemically separates oxygen gas because they can be driven only by the oxygen partial pressure difference across the membrane at high temperatures without connecting to external circuits [3,4]. Figure 1 shows the mechanism of the oxygen separation process of the oxygen separation membrane, oxygen molecules in the air dissociate on the surface of the membrane to generate oxide ions on the high oxygen partial pressure side or feed side, then the oxide ions diffuse from the feed side through the lattice vacancies in the crystal structure to the low oxygen partial pressure side or permeation side, then recombine to form oxygen molecules. In this process, electrons are transported in the opposite direction of the oxygen transport path to balance the charge neutrality [5]. Important requirements for membrane material selection are a high oxide ion conductivity, chemical stability, and high mechanical strength. Oxide-ion conductors with the structure of fluorite (AO_2) and perovskite (ABO_3) meet these requirements [6,7]. MIECs are commonly used as single-phase oxygen separation membranes [8]. $Ba_{0.5}Sr_{0.5}Co_{0.8}Fe_{0.2}O_{3-\delta}$ (BSCF), which has both a high ionic and electronic conductivity, has the highest oxygen permeability of all MIEC ceramic materials [9,10]. To further improve the oxygen separation properties, it is not enough to just look for new MIEC materials as the diffusion rate of oxide ions in the MIEC-based single-phase membrane is almost at its limit.

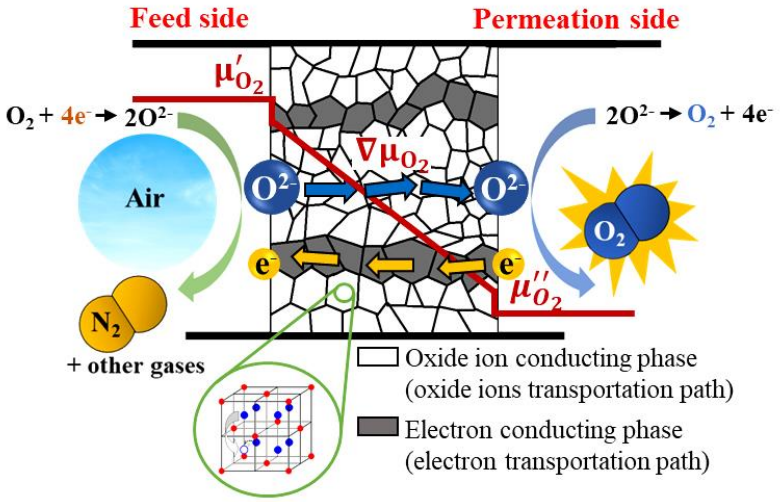

Figure 1 Schematic illustration of dual-phase membrane.

In this research study, attention is being paid to a dual-phase membrane. A dual-phase membrane is a composite material consisting of an oxide ion-conducting phase as the oxide ions' transportation path and an electron-conducting phase as an electron transportation path [11,12]. As shown in Figure 1, by separating the transport paths of the oxide ions and electrons, it is possible to obtain a membrane that can achieve a high conductivity of both the oxide ions and electrons. Eight mol% yttria-stabilized zirconia (8YSZ) is an excellent oxide-ion conductor with a fluorite structure [13]. It is suitable for use as an oxide ion conductive phase in a dual-phase membrane [14]. Carbon and metals with a high electron conductivity are suitable for the electron conduction phase [15,16]. Most conventional methods for producing a dual-phase membrane are prepared by a solid phase reaction method [17,18] in which different types of powders are simply mixed and sintered. However, it is difficult to achieve both the percolation structures of the oxide ion conduction phase and the electron conduction phase. Therefore, a new method is necessary to realize the co-continuous structure of the two phases for improvement of the separation performance. In this study, a new and simple manufacturing process of a dual-phase membrane by filling an oxide ion conductive phase material in the pores of an electron conductive phase material with a three-dimensional network structure is presented.

2. Experimental procedures

The microstructure of carbon felt and nickel foam are shown in Figures 2(a) and 2(b). The continuous porous structure which lead to the continuous transportation of electrons exhibited a high electronic conductivity.

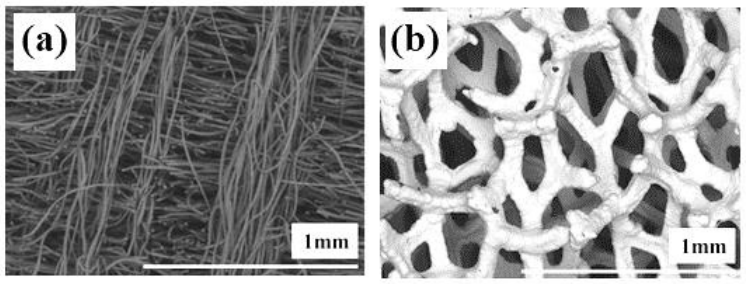

Figure 2 Microstructure of (a) carbon felt and (b) nickel foam.

A schematic showing the preparation process of the YSZ-based dual phase membranes is shown in Figure 3. Eight mol% yttria-doped zirconia powders (TZ-8Y (D_{50}: 0.6 μm) and TZ-8YS (D_{50}: 0.6 μm), Tosoh, Tokyo, Japan), 30 vol% TZ-8Y and 40 vol% TZ-8YS were dispersed in distilled water with 2 wt% ammonium polyacrylate as a dispersant (Alon-A6114, Tosoh) to prepare the suspensions. The carbon felt and nickel foam were cut into a 20-mm diameter disk shape with a thickness of 3 mm and placed in distilled water followed by evacuation for 30 minutes to remove all the gas inside the porous structure, then the YSZ suspension was vacuum impregnated to form the green composite bodies. After roughening the green samples by sandpaper, the green samples were cold isostatically pressed at 350 MPa for 10 minutes, thus achieving the uniform packing of the YSZ particles inside the porous structure. The green samples were sintered by two types of sintering processes which are the conventional sintering process under an Ar atmosphere and spark plasma sintering in a vacuum atmosphere (SPS, LaboxTM-325 Sinter Land Inc., Tokyo, Japan). SPS is a high pulse direct current technique to densify the sample at a low sintering temperature and short sintering time [19]. The YSZ-carbon felt and the YSZ-nickel foam dual-phase membranes were sintered at different temperatures taking into account the melting points of the carbon felt and the nickel foam. The SPS was performed at the pressure of 80 MPa for 10 minutes. By using this new fabrication technique, a continue phase structure would be formed with a simple, low cost and low energy consumption.

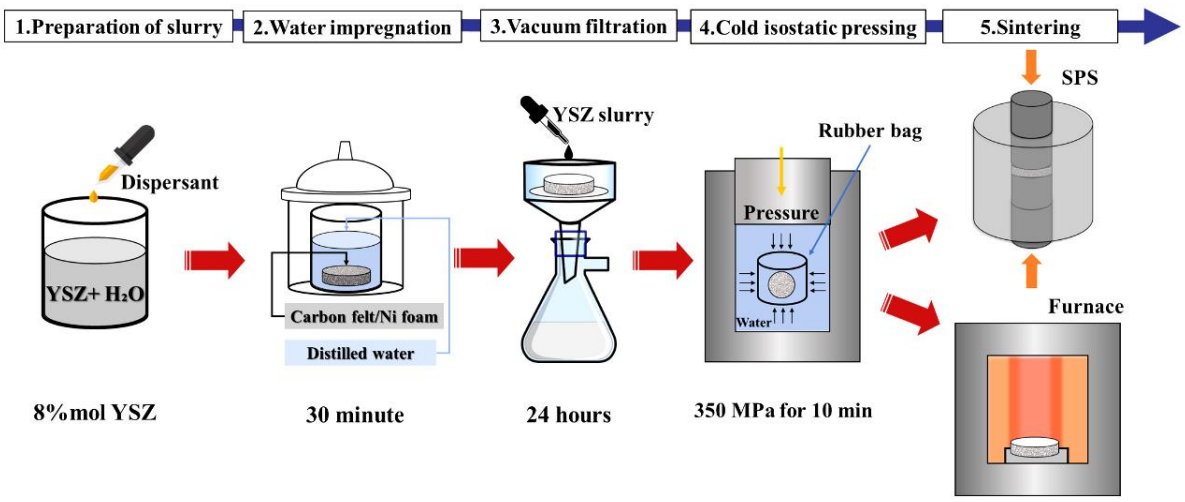

Figure 3 Schematic showing the preparation process of YSZ-based dual-phase membranes.

The phase stability and chemical compatibility of the dual-phase membranes fabricated at the different sintering temperatures were investigated. The sintered samples were ground in an agate mortar and examined by X-ray diffraction (XRD, Miniflex 600 Rigaku Co., Ltd., Tokyo, Japan), The XRD patterns were obtained with a step of 0.2 deg, speed of 10 deg/min at 40 kV and 15 mA. The microstructure of the dual-phase membranes was observed by a scanning electron microscope (SEM, JEOL JSM-5600LV (JEOL Pte Ltd., Tokyo, Japan) at a 5 kV accelerating voltage. Finally, an oxygen separation test was performed using the selected sample [1].

3. Results and discussion

In this experiment, two types of YSZ powders (TZ-8Y and TZ-8YS) were used as mentioned in the experimental procedures. The company's catalog states that TZ-8Y has a smaller primary particle size and is easier to sinter than TZ-8YS; therefore, it was postulated that TZ-8Y could be densified at lower temperatures. However, the solid concentration of the highly-fluid suspensions was approximately 30 vol% and 40 vol% for TZ-8Y and TZ-8YS, respectively, even when the amount of the dispersant was optimized. The specific surface areas of TZ-8Y and TZ-8YS are 16 m^2/g and 7 m^2/g respectively. This difference is reasonable considering that TZ-8Y has more particle-to-particle interactions and is more likely to agglomerate than TZ-8YS. It was difficult to fill the voids of the carbon felt or nickel foam with the agglomerated powder, and only low-density compacts were obtained as shown in Figure 4, resulting in the requirement of a higher temperature for densification. Therefore, TZ-8YS was used for the preparation of the membrane.

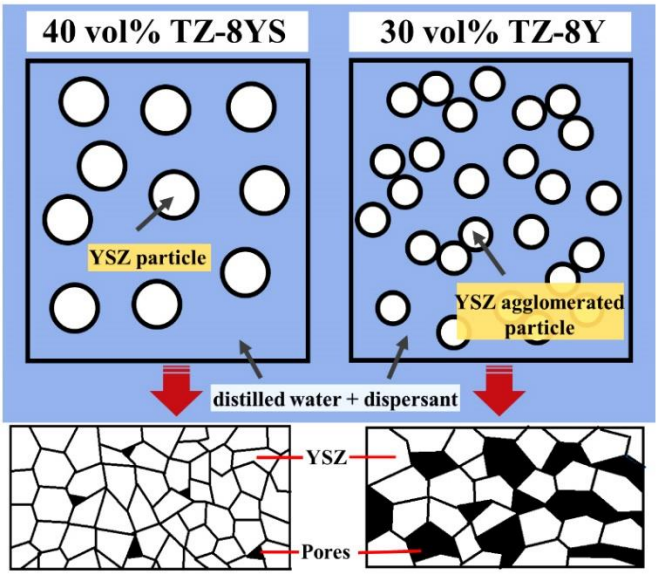

Figure 4 Illustration of YSZ slurry with two kinds of YSZ powders.

Figure 5(a) shows the microstructure of the YSZ-carbon felt dual-phase membrane prepared from TZ-8Y. The sample sintered at 1600 °C has a relative density of only 85.91%, and small particles can be seen around it. Compared to the microstructure of the YSZ-carbon felt dual-phase membrane prepared from TZ-8YS in Figure 5(b), the sample sintered at the same temperature was more dense with a relative density of 95.03%.

Figure 5(c) shows the microstructure of the YSZ nickel foam dual-phase membrane prepared from TZ-8Y sintered at 1200 °C Results similar to the YSZ carbon felt dual-phase membrane were obtained. The YSZ part was not densified and its density was only 84.05%. On the other hand, when TZ-8YS was used as the raw material, the YSZ part had a high density, and its relative density reached 90.83% as shown in Figure 5(d).

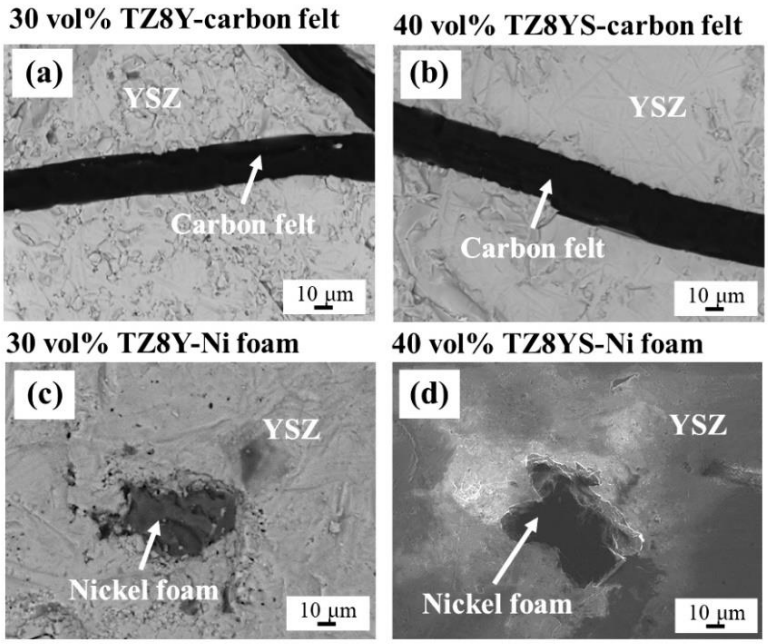

Figure 5 The microstructure of (a) 30 vol% TZ8Y, (b) 40 vol% TZ8YS of YSZ-carbon felt dual-phase membrane sintered by SPS at 1600 °C, (c) 30 vol% TZ8Y, and (d) 40 vol% TZ8YS of YSZ-nickel foam dual-phase membrane sintered by SPS at 1200 °C.

Achieving a gas-tight dense structure is one of the requirements to fabricate the oxygen separation membrane without leaking nitrogen gas on the permeation side. The dense packing of the YSZ particles would increase the transportation path of the oxygen ions. The YSZ sintered sample with a low packing could lead to gas leaking in addition to a low oxygen transportation. To achieve a gas-tight dense membrane, the sintering process should be optimized. The effects of the sintering process on the microstructure and density of the sintered samples were characterized. The sample sintered at 1600 °C for the YSZ-carbon felt dual-phase membrane was fabricated by SPS in a vacuum and the conventional sintering process in argon atmosphere were investigated. In the case of the YSZ-nickel foam dual-phase membrane, it was possible to sinter at 1400 °C by the conventional sintering, but in the case of SPS, the pulse current flows intensively to the nickel in the sample during sintering, and the nickel melts at sintering temperatures higher than 1200 °C. Therefore, the sintered sample at 1200 °C for the YSZ-nickel dual-phase membrane was produced by SPS.

Figure 6(a) compares the microstructure of the YSZ-carbon felt dual-phase membrane sintered by SPS and the conventional sintering process. The samples sintered by SPS have a good attachment between the YSZ and carbon felt. Small, flaky YSZ crystals were observed in the samples sintered by the conventional sintering process, and the relative density decreased of the green compact density to 23.9%. Figure 6(b) compares the microstructures of the YSZ-nickel foam dual-phase membrane sintered by SPS and the conventional sintering process. The microstructures of the samples sintered by these two sintering processes have a good attachment between the YSZ and nickel foam. However, the use of the conventional sintering process strongly affects the sample size. The sintered body produced by the conventional sintering method had a high relative density similar to that of the SPS sintered body and achieved a shrinkage rate of 16.6%, but the sample was warped and was not suitable for oxygen separation. As a result, the spark plasma sintering process clearly enhanced the densification in the YSZ-based dual-phase membrane with a high structural stability. Thus, the SPS process is a promising technique for the sintered membrane in this research study.

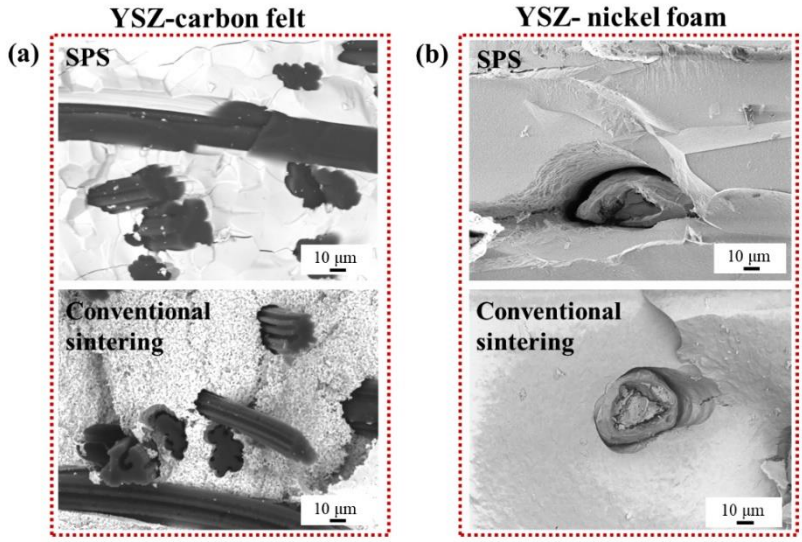

Figure 6 The microstructure of (a) YSZ-carbon felt dual-phase membrane sintered at 1600 °C by SPS and conventional sintering and (b) YSZ nickel foam dual-phase membrane sintered at 1200 °C by SPS and 1400 °C conventional sintering.

Based on the above results, the TZ-8YS was used as the YSZ source for preparing the YSZ suspension. For the sintering process, SPS was selected to achieve the gas tight dense membrane. After the sintering process, the YSZ-carbon felt dual-phase membrane and YSZ-nickel foam dual-phase membrane were successfully fabricated by SPS without any apparent cracking. The relationship between the relative density and sintering temperature of the sintered samples is shown in Figure 7. The relative density of the YSZ-carbon felt dual-phase membrane can be achieved up to 95% at the sintering temperature of 1600 °C. For the YSZ-nickel foam dual-phase membrane, the space inside the nickel foam is larger than the carbon felt, and the YSZ powder would be filled in larger amounts than the carbon felt. The relative density of 90% can be achieved at the sintering temperature of 1200 °C for the YSZ-nickel foam dual-phase membrane.

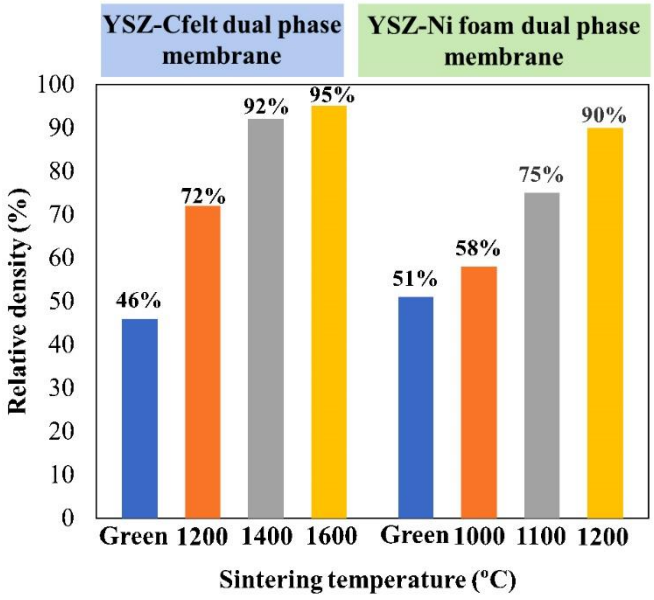

Figure 7 Relative density of YSZ-based dual-phase membranes by SPS at different sintering temperatures.

Figure 8 shows the XRD pattern of the YSZ-carbon felt membrane sintered by SPS. The XRD patterns of the sintered samples at 1200 and 1400 °C indicated that the sintered sample consisted of YSZ and graphite, suggesting that there is no reaction between the YSZ and carbon felt at the sintering temperatures below 1400 °C. When the temperature was raised to 1600 °C, small peaks of zirconia carbide, which is the secondary phase, were observed. This secondary phase suggested the strong bond between the YSZ and carbon felt sintered at a high temperature.

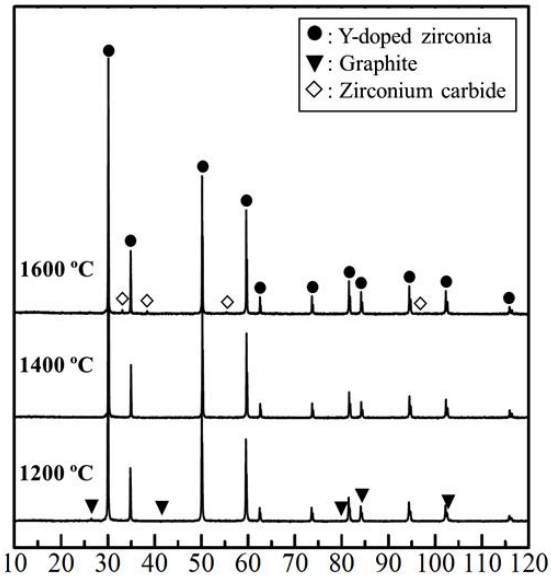

Figure 8 XRD patterns of YSZ-carbon felt membrane sintered at 1200, 1400 and 1600 °C by SPS.

Figure 9 shows the XRD patterns of the YSZ-nickel foam dual-phase membrane sintered at 1000, 1100 and 1200 °C. The phase composition of the YSZ-nickel foam dual-phase membrane was yttria doped zirconia and nickel at all the performed sintering temperatures. The YSZ and nickel did not react at all the sintering temperatures suggesting a high phase stability between these two phases.

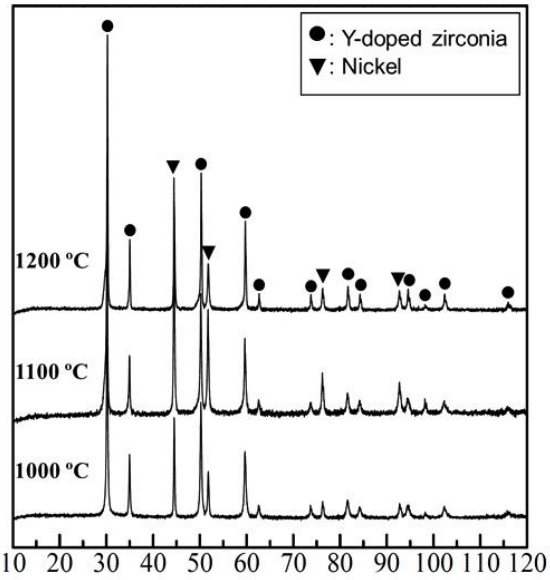

Figure 9 XRD patterns of YSZ-nickel foam membrane sintered at 1000, 1100 and 1200 °C by SPS.

Figure 10 shows a SEM image of the microstructure of the YSZ-carbon felt dual-phase membrane sintered at 1200, 1400 and 1600 °C. This shows that the two phases in the membrane were tightly attached. Since there are no voids between the two phases, it can be assumed that no gas leaks will occur during the air separation process. The microstructure of the YSZ-nickel foam two-phase film is shown in Figure 11. A structure in which the two phases were tightly attached was observed at a sintering temperature higher than 1100 °C.

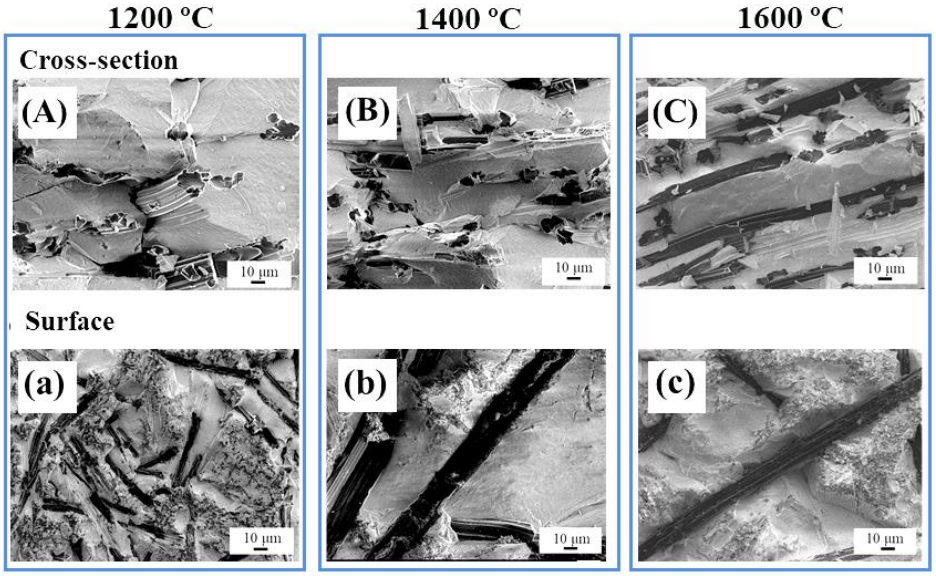

Figure 10 Surface and cross section images of the microstructures of YSZ-carbon felt dual-phase membranes sintered at (A) and (a) 1200 °C, (B) and (b) 1400 °C, and (C) and (c) 1600 °C.

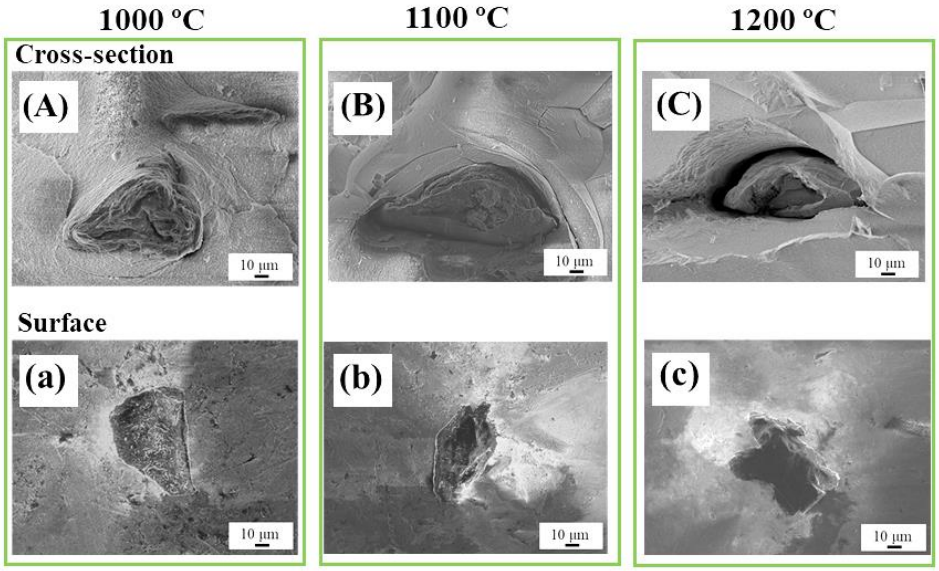

Figure 11 Surface and cross section images of the microstructures of YSZ-nickel foam dual-phase membranes sintered at (A) and (a) 1000 °C, (B) and (b) 1100 °C, and (C) and (c) 1200 °C.

Finally, the selected sample, which was the YSZ-nickel foam dual-phase membrane sintered at 1200 °C, exhibited an oxygen permeation flux of 0.21 ml/min.cm² that was obtained at 800 °C. Further improvement of the oxygen separation performance of the YSZ-based dual phase membrane will be developed for future research.

4. Conclusions

YSZ-carbon felt and YSZ-nickel foam dual-phase membranes using TZ-8YS powder as a YSZ source were successfully fabricated by SPS with a good phase stability and high chemical compatibility. The relative density of 95% could be obtained with YSZ-carbon felt dual-phase membrane sintered at 1600 °C and the relative density of 90% could be obtained with the YSZ-nickel foam dual-phase membrane sintered at 1200 °C. In case of the YSZ-carbon felt dual-phase membrane, the XRD results revealed the appearance of zirconia carbide when sintered at 1600 °C due to the strong attachment between the two phases. For the XRD results of the YSZ-nickel foam dual-phase membranes, no reaction between the YSZ and nickel foam was observed at the sintering temperatures between 1000 to 1200 °C. A tight attachment was achieved by the YSZ-carbon felt dual-phase membranes at the performed temperatures and the YSZ-nickel foam dual-phase membranes at the sintering temperature up to 1100 °C. Finally, the YSZ-nickel foam dual-phase membrane sintered at 1200 °C was chosen for an oxygen separation performance test. The highest oxygen permeation flux of 0.21 ml/min·cm² was obtained at 800 °C. The improved oxygen separation performance of the YSZ-based dual phase membrane will be achieved in near future research.

Acknowledgment

The authors would like to thank the engineers, Ms. Eriko Suzuki (NIMS), Ms. Chiho Togashi (NIMS) and Mr. Koji Nakazato (NIMS), for their technical support for preparing the porous materials.

References

[1] K. Ishii, C. Matsunaga, K. Kobayashi, Fabrication of BSCF-based mixed ionic-electronic conducting membrane by electrophoretic deposition for oxygen separation application, *J. Eur. Ceram. Soc.* **39** (2019) 5292-5297.

[2] B. Adhikari, C. J. Orme, Technoeconomic analysis of oxygen-nitrogen separation for oxygen enrichment using membranes, *Sep. Purif. Technol.* **268** (2021) 118703.

[3] I. Riess, Mixed ionic–electronic conductors-material properties and applications, *Solid State Ion.* **157** (2003) 1-17.

[4] S. S. Hashim, A. R. Mohamed, Oxygen separation from air using ceramic-based membrane technology for sustainable fuel production and power generation, *Renew. Sust. Energ. Rev.* **15** (2011) 1284-1293.

[5] S. P. S. Badwal, F. T. Ciacchi, Ceramic membrane technologies for oxygen separation, *Adv. Mater.* **13** (2001) 993-996.

[6] J. Sunarso, S. Baumann, Mixed ionic-electronic conducting (MIEC) ceramic-based membranes for oxygen separation, *J. Membr. Sci.* **320** (2008) 13-41.

[7] C. Chatzichristodoulou, P. Norby, P. V. Hendriksen, Size of oxide vacancies in fluorite and perovskite structured oxides, *J. Electroceram.* **34** (2015) 100-107.

[8] Y. Lin, S. Fang, D. Su, Enhancing grain boundary ionic conductivity in mixed ionic-electronic conductors, *Nat. Commun.* **6** (2015) 6824.

[9] S. Baumanna, F. Schulze-Küppersa, S. Roitschc, Influence of sintering conditions on microstructure and oxygen permeation of $Ba_{0.5}Sr_{0.5}Co_{0.8}Fe_{0.2}O_{3-\delta}$ (BSCF) oxygen transport membranes, *J. Membr. Sci.* **359** (2010) 102-109.

[10] K. Ishii, C. Matsunaga, K. Kobayashi, Fabrication of BSCF-based mixed oxide ionic-electronic conducting multi-layered membrane by sequential electrophoretic deposition process, *J. Eur. Ceram. Soc.* **41** (2021) 2709-2715.

[11] F. Schulze-Kuppers, S. Baumann, Manufacturing and performance of advanced supported $Ba_{0.5}Sr_{0.5}Co_{0.8}Fe_{0.2}O_{3-\delta}$ (BSCF) oxygen transport membranes, *J. Membr. Sci.* **433** (2013) 121-125.

[12] Z. Zhang, W. Zhou, Novel approach for developing dual-Phase ceramic membranes for oxygen separation through beneficial phase reaction, *ACS Appl. Mater. Interfaces.* **7** (2015) 22918-22926.

[13] H. Wang, W. S. Yang, Y. Cong, Structure and oxygen permeability of a dual-phase membrane, *J. Membr. Sci.* **224** (2003) 107-115.

[14] A. V. Joshi, J. J. Steppan, Solid electrolyte materials, devices, and applications, *J. Electroceram.* **13** (2004) 619-625.

[15] D. Panthi, N. Hedayat, Densification behavior of yttria-stabilized zirconia powders for solid oxide fuel cell electrolyte, *J. Adv. Ceram.* **7** (2008) 325-335.
[16] T. X. Huong, M. Bechelany, Carbon felt based-electrodes for energy and environmental applications: A review, *Carbon* **122** (2017) 564-591.
[17] N. K. Chaudhari, H. Jin, Nanostructured materials on 3D nickel foam as electrocatalysts for water splitting, *Nanoscale* **9** (2017) 12231-12247.
[18] X. Zhu, H. Wang, W. Yang, Relationship between homogeneity and oxygen permeability of composite membranes, *J. Membr. Sci.* **309** (2008) 120-127.
[19] X. J. Chen, K. A. Khor, Overcoming the effect of contaminant in solid oxide fuel cell (SOFC) electrolyte: Spark plasma sintering (SPS) of 0.5 wt.% silica-doped yttria-stabilized zirconia (YSZ), *Mater. Sci. Eng. A* **374** (2004) 64-71.